DOI: 10.1007/s11099-016-0669-9 PHOTOSYNTHETICA 55 (4): 568-578, 2017

Comparative analysis of ultrastructure, antioxidant enzyme activities, and photosynthetic performance in rice mutant 812HS prone to photooxidation

J. MA[*], C.F. LV[*], B.B. ZHANG[*], F. WANG[*], W.J. SHEN[*], G.X. CHEN[*], Z.P. GAO[*,+] and C.G. LV[**,+]

School of Life Sciences, Nanjing Normal University, Nanjing 210023, China[*]
Institute of Food and Crops, Jiangsu Academy of Agricultural Sciences, Nanjing, 210014, China[**]

Abstract

Under optimal conditions, most of the light energy is used to drive electron transport. However, when the light energy exceeds the capacity of photosynthesis, the overall photosynthetic efficiency drops down. The present study investigated the effects of high light on rice photooxidation-prone mutant 812HS, characterized by a mutation of leaf photooxidation 1 gene, and its wild type 812S under field conditions. Our results showed no significant difference between 812HS and 812S before exposure to high sunlight. However, during exposure to high light, shoot tips of 812HS turned yellow and their chlorophyll (Chl) content decreased. Transmission electron microscopy showed that photooxidation resulted in significant damage of chloroplast ultrastructure. It was confirmed also by inhibited photophosphorylation and reduced ATP content. The decreased coupling factor of ATP, Ca^{2+}-ATPase and Mg^{2+}-ATPase activities also verified these results. Further, significantly enhanced activities of antioxidative enzymes were observed during photooxidation. Malondialdehyde, hydrogen peroxide, and the superoxide generation rates also increased. Chl *a* fluorescence analysis found that the performance index and maximum quantum yield of PSII declined on August 4, 20 days after high-light treatment. Net photosynthetic rate also decreased and substomatal CO_2 concentration increased in 812HS at the same time. In conclusion, our findings indicated that excessive energy triggered the production of toxic reactive oxygen species and promoted lipid peroxidation in 812HS plants, causing severe damage to cell membranes, degradation of photosynthetic pigments and proteins, and ultimately inhibition of photosynthesis.

Additional key words: malondialdehyde; photophosphorylation; proteins; reactive oxygen species.

Introduction

Efficient photosynthesis is a key for plant survival and fitness (Long *et al.* 1983). Under normal conditions, most of the light energy is used to drive electron transport. However, when the light energy exceeds the capacity of photosynthesis, it can activate a production of the singlet oxygen state ($^1O_2$) (Szabó *et al*. 2005). Singlet oxygen molecules and other forms of reactive oxygen species (ROS) cause oxidative damage to pigments, proteins, and lipids in the thylakoid membrane, ultimately, weakening the overall photosynthetic efficiency. Persistent photoinhibition triggers photooxidation which results in damage to photosynthetic apparatus.

In addition, aldehyde products of lipid peroxidation were defined as evidence of oxidative stress (Sandalio *et al*. 2001). Disruption of redox homeostasis in cells and rapid induction of ROS, such as superoxide ($O_2^{\cdot-}$), hydroxyl radical ($^{\cdot}OH$), and hydrogen peroxide (H_2O_2), which damage membrane lipids, proteins, nucleic acids, and Chl, result in the irreparable damage to photosynthetic organs, degradation of photosynthetic pigments,

Received 26 April 2016, *accepted* 2 September 2016, *published as online-first* 26 October 2017.
[+]Corresponding authors; phone: +862585891079, fax: +862585898223, e-mail: majing129@126.com, lvchuangen@sina.com.
Abbreviations: AA – ascorbate; APX – ascorbate peroxidase; BSA – bovine serum albumin; CAT – catalase; Chl – chlorophyll; C_i – substomatal CO_2 concentration; DAB – 3,3-diaminobenzidine; FM – fresh mass; F_V/F_M – maximal quantum yield of PSII; GR – glutathione reductase; MDA – malondialdehyde; NBT – nitroblue tetrazolium; $O_2^{\cdot-}$ – superoxide; $^{\cdot}OH$ – hydroxyl radical; PI_{ABS} – performance index; P_N – net photosynthetic rate; POD – guaiacol peroxidase; RC – reaction centers; ROS – reactive oxygen species; SOD – superoxide dismutase; TBA – thiobarbituric acid; TEM – transmission electron microscopy.
Acknowledgments: Studies in the Chen Laboratory were supported by the National Natural Science Foundation of China (Grant. No. 31271621/C1302, and No. 31671663), Project BK20140916 supported by NSF of Jiangsu Province of China, Program of Natural Science Research of Jiangsu Higher Education Institutions of China (Grant. No.14KJB180011), and a Project Funded by the Priority Academic Program Development of Jiangsu Higher Education Institutions and Jiangsu Collaborative Innovation Center for Modern Crop Production.

metabolic dysfunction, and even cell death (Shah *et al*. 2001, Blokhina *et al*. 2003, Szabó *et al*. 2005, Sharma and Dubey 2007). In order to quench ROS and overcome oxidative stress, plants are equipped with antioxidative defense systems comprising superoxide dismutase (SOD, EC 1.15.1.1), guaiacol peroxidase (POD, EC 1.11.1.7), catalase (CAT, EC 1.11.1.6), and enzymes of ascorbate-glutathione cycle, such as ascorbate peroxidase (APX, EC 1.11.1.11) and glutathione reductase (GR, EC.1.6.4.2). The induction of ROS scavenging enzymes constitutes an important protective mechanism which can serve as a biomarker reflecting an antioxidative capacity and photo-oxidation tolerance (Fang *et al*. 2008). SOD is the enzyme of the first defense against oxidative stress, and consists of a group of metallo-isoenzymes that neutralize O_2^- to produce H_2O_2 and O_2^-. CAT detoxifies H_2O_2 generated in glyoxysomes and peroxisomes (Gratão *et al*. 2005). POD utilizes H_2O_2 and oxidizes various substrates in the cell. In chloroplasts, APX catalyzes the conversion of H_2O_2 to H_2O utilizing ascorbate (AA). During regeneration of AA in chloroplasts, enzymes of the ascorbate-glutathione cycle play a significant role (Nakano and Asada 1987). Altered antioxidative defense system is the focus of current research against photooxidation, with less information available in cereal crops, especially, in rice (Phung and Jung 2015). In addition, most of the photooxidation mutants were artificially induced. Zhou *et al*. (2013) used a yellow-leaf mutant *lyl1-1*, which was isolated from the progeny of Japonica rice ZH11 treated with ^{60}Co. They found that the *lyl1-1* mutant suffered from severe photooxidative damage and displayed a drastic reduction in the contents of α-tocopherol and photosynthetic proteins. They concluded that *LYL1* gene plays an important role in response to high light intensity in rice.

A mutant of two-line sterile rice, 812HS, showed leaf photooxidation during a tillering and jointing stage. There were no significant differences in agronomic traits between 812HS and wild type, 812S. Before rainy season, the phenotypes of 812HS and 812S exhibited no difference. After rainy season, the leaves of 812HS seedlings showed etiolation, especially, at leaf tips, while the leaves of 812S were green. PSII reaction centers and PSII electron transport of the mutant were significantly affected in comparison with the wild type (Lai *et al*. 2012). Genetic analysis and gene mapping showed that the trait was controlled by a new dominant gene, leaf photooxidation 1 (*LPO1(t)*) on chromosome 4 located between RM5414 and RM401 (Lai *et al*. 2012). The mutant exhibited molecular mechanism of leaf photooxidation which was important to alleviate the photooxidation in rice.

This study investigated the response of 812HS and 812S to natural light and shade by measuring (*1*) changes in photosynthetic pigments and chloroplast ultrastructure; (*2*) changes in photosynthesis and soluble protein content; (*3*) changes in malondialdehyde (MDA), O_2^-, and H_2O_2 content; and (*4*) changes in SOD, POD, CAT, APX, and GR activities. We investigated the factors underlying the oxidation phenomena in 812HS and formulated a theory for further study of its molecular mechanism.

Materials and methods

Plant materials and growth conditions: Experiments were carried out at the experimental fields of Xianlin campus, Nanjing Normal University, Nanjing, China. During the period from 1 June (22 d before the first sampling) to 15 September (the last sampling date), the mean, maximal, and minimum daily temperatures were 26.63 ± 0.11°C, 34.1 ± 0.14°C, and 19.25 ± 0.28°C, respectively. The daily relative humidity was 79.3 ± 0.9%. Plants were grown in a field in May 2014. N fertilizer (3,375 kg ha^{-1}) was applied, with an N-P-K ratio of 1:0.6:0.6. Plants were watered and fertilized regularly during the growing season. The photooxidative mutant 812HS was isolated from the progeny of Japonica rice 812S. At the seedling stage, the leaves of 812S and 812HS were uniform. At the tillering and jointing stages, the tips of 812HS leaves showed photooxidation after rainy season. Leaves were collected separately, frozen immediately in liquid nitrogen, and stored at −80°C. The experiments were performed in triplicate. We also carried out a shading experiment. A black integument covered the plants of 812S and 812HS in order to reach about 65% of natural light at rice canopy, which was PPFD of 600–800 μmol m^{-2} s^{-1} during the growing season. As controls, the plants were also growing under natural light. The plants were all potted with the rate of three seedlings per pot of diameter 18 mm.

Pigment content: The contents of Chl as well as the Chl *a*/*b* ratio were determined according to a previous study (Wu *et al*. 2007). Pigments were extracted by grinding leaves in ice-cold 80% (v/v) acetone. The extract was centrifuged at 3,000 × *g* for 5 min. The absorbance of the supernatant was measured at 470, 645, and 663 nm with a *UV-754* spectrophotometer (*Zealquest Scientific,* Shanghai, China). Pigment contents were calculated in μg g^{-1}(fresh mass, FM).

Chloroplast ultrastructure: The leaves of 812S and 812HS without the midribs were cut into small pieces and fixed for 2 h at 4°C in 2.5% (v/v) glutaraldehyde in 0.1 M phosphate buffer solution (PBS, pH = 7.3), and post-fixed in 5% (w/v) aqueous osmium tetraoxide for 2 h. The fixed samples were dehydrated in an ascending ethanol gradient, and finally embedded in *Epon 812* resin. Thin sections were cut using an *LKB-V* ultramicrotome (*LKB Ultrascan XL*, Bromma, Sweden) and double stained in 2% (w/v) uranyl acetate and lead citrate before examination under a *Hitachi 600-A-2* transmission electron microscope (TEM)

(*Hitachi*, Tokyo, Japan) operating at 75 kV.

Histochemical localization of $O_2^{\cdot-}$ and H_2O_2: The localization of $O_2^{\cdot-}$ *in situ* was performed by monitoring the formazan precipitation in the nitroblue tetrazolium (NBT) reaction with $O_2^{\cdot-}$ according to the method of Rossel *et al*. (2007). Leaves were washed before pre-immersion in 6 mM NBT in 10 mM Na-citrate buffer, pH = 6. After exposure, the leaves were immersed in boiling ethanol for 15 min to remove Chl and then rehydrated in 40% glycerol and mounted on glass slides. Dark blue insoluble formazan was produced by the reaction of NBT with $O_2^{\cdot-}$. The same procedure was repeated for H_2O_2, which was detected by the formation of dark brown spots when 3,3-diaminobenzidine (DAB, 1 mg ml^{-1}, pH = 3.8) reacted with H_2O_2. Each experiment was repeated at least three times using different plants, and multiple leaves per plant were examined.

Determination of $O_2^{\cdot-}$ and H_2O_2: The generation rate of $O_2^{\cdot-}$ was monitored by the nitrite formation from hydroxylamine according to Shen *et al*. (2015). After being homogenized in 3 ml of 65 mM K-phosphate buffer (pH = 7.8), 0.2 g of plant material was centrifuged at 5,000 × *g* for 10 min at 4°C. The supernatants (750 µl) were mixed with 675 µl of the above phosphate buffer and 75 µl of 10 mM hydroxylamine chlorohydrate. After incubation, 500 µl of mixture was added to 500 µl of 17 mM sulfanilamide and 500 µl of 7 mM α-naphthylamine and the mixture was incubated again before being added to the same volume of ether. The mixture was centrifuged at 1,500 × *g* for 5 min. Absorbance of aqueous phase was measured at 530 nm and $O_2^{\cdot-}$ production rates were calculated from the standard curve of $NaNO_2$. The results were expressed in µmol(nitrite) g^{-1}(FM).

The H_2O_2 content was determined according to Hossain *et al*. (2010) by monitoring titanium sulfate after homogenization of 0.5-g samples with phosphate buffer (50 mM, pH = 6.8) and centrifugation. The supernatants were then mixed with 0.1% (w/v) $TiCl_4$ in 20% (v/v) H_2SO_4, and the mixture was centrifuged at 6,000 × *g* for 15 min. The absorbance was measured at 410 nm by the spectrophotometer (*Cintra 1010*, *GBC*, Australia) and H_2O_2 amounts were read off the standard curve. The results were expressed in mmol g^{-1}(FM).

MDA: Lipid peroxidation was determined in terms of MDA content using thiobarbituric acid (TBA) reaction according to Shen *et al*. (2015). Leaves were homogenized in 10% (w/v) trichloroacetic acid (TCA) solution and centrifuged at 5,000 × *g* for 10 min. The resulting supernatant was mixed with the same volume of 0.5% (w/v) TBA solution in 20% (w/v) TCA. The mixture was then heated at 100°C for 30 min and quickly cooled on ice. The absorbance was measured at 532 nm and 600 nm at 25°C (*Cintra 1010*, *GBC*, *Australia*), and the concentration of MDA was expressed in nmol g^{-1}(FM).

Activities of antioxidant enzymes: After homogenizing 0.5 g of plant material in 0.05 M PBS, and centrifugation at 10,000 × *g* for 20 min at 4°C, the supernatant was used to determine activities of SOD, CAT, and POD (Fu *et al*. 2014). Enzyme activity assays were performed in 3-ml reaction volumes at 25°C and determined spectrophotometrically (*Cintra 1010*, *GBC*, Australia).

SOD activity was measured according to Stewart and Bewley (1980). The reaction mixture included 50 mM phosphate buffer (pH = 7.8), 13 mM methionine, 75 mM nitroblue tetrazolium (NBT), 0.1 mM EDTA, 50 mM Na_2CO_3, and 100 µl of enzyme extract. The reaction was allowed to proceed for 15 min under illumination of two 20-W fluorescent tubes. Absorbance of the reaction mixture was read at 560 nm. One unit of activity was defined as the amount of enzyme required to inhibit 50% of the initial reduction of NBT under light. Enzyme activity was expressed as unit g^{-1}(FM).

POD activity was assayed by monitoring the formation of tetraguaiacol at 470 nm (ε = 26.6 mM^{-1} cm^{-1}) according to the Fu *et al*. (2014). A reaction mixture consisted of 16 mM guaiacol, 0.15 M phosphate buffer (pH = 6.1), 2 mM H_2O_2, and 100 µl of enzyme extract. Enzyme activity was expressed in mmol(tetraguaiacol) min^{-1} g^{-1}(FM).

CAT activity was measured spectrophotometrically at 240 nm by the decomposition of H_2O_2 according to Fu *et al*. (2014). A assay mixture was set up with 50 mM phosphate buffer (pH = 7), 15 mM H_2O_2, and 100 µl of enzyme extract. One unit of CAT activity was defined in nmol(H_2O_2) min^{-1} g^{-1}(FM) at 25ºC.

APX activity was determined by the rate of ascorbate oxidation to dehydroascorbate at 285 nm (ε = 2.8 mM^{-1} cm^{-1}) according to the procedure of Rao *et al*. (1996). About 1 g of leaves was homogenized in 100 mM phosphate buffer (pH = 7.5) containing 5 mM ascorbate and 1 mM EDTA at 4ºC, filtered, and centrifuged. The reaction mixture consisted of 50 mM potassium phosphate buffer (pH = 7.5), 0.5 mM ascorbate, and 0.3 mM H_2O_2, and 50 µl of enzyme extract. Enzyme activity was expressed in µmol (ascorbate) min^{-1} g^{-1}(FM).

GR activity was determined by recording glutathione-dependent oxidation of NADPH at 340 nm (ε = 6.2 mM^{-1} cm^{-1}) according to Shen *et al*. (2015) with slight modifications. The assay volume included 0.1 mM Tris buffer, 5 mM glutathione oxidized (GSSG), and 600 µl of the extract. The reaction was initiated by the addition of 0.1 mM NADPH. The GR activity was expressed in µmol(NADPH) min^{-1} g^{-1}(FM).

Photophosphorylation, ATP content, Ca^{2+}-ATPase and Mg^{2+}-ATPase activities: Chloroplasts were isolated as described by Ketcham *et al*. (1984) and Chen *et al*. (2004) with minor modifications. Plant material (5 g) was cut into pieces and grinded in the extraction medium (50 mM Tris-HCl, pH = 7.6, 5 mM $MgCl_2$, 10 mM NaCl, 0.4 M sucrose, and 0.1% bovine serum albumin, BSA). The homogenate was filtered and centrifuged at 1,000 × *g* for 2 min. The

supernatant was re-centrifuged at 2,000 × *g* for 2 min. After removal of the supernatant, the precipitate was supplemented with the extraction medium and the tube was slightly rotated on ice blocks in order to obtain a uniform suspension of chloroplasts which was then stored in the dark on ice for use in subsequent procedures.

The photophosphorylation activity was measured using a luminescence meter (*FG-300*, *Thermo*, Shanghai, China) according to Ketcham *et al*. (1984) and expressed as μmol(ATP) mg^{-1}(Chl) h^{-1}. The ATP content was measured using the bioluminescence method as described by Zhu *et al*. (2001) and expressed as μmol(ATP) mg^{-1}(Chl). Ca^{2+}-ATPase and Mg^{2+}-ATPase activities were measured as described by Vallejos *et al*. (1983). Enzyme activity was expressed in μmol(Pi) mg^{-1}(Chl) h^{-1}.

Gas exchange: Net photosynthetic rate (P_N) and substomatal CO_2 concentration (C_i) were measured by a portable photosynthesis system (*Ciras 2*, *PP System*, UK). Experiments were performed between 10:00 and 12:00 h, carried out in triplicates, where each replicate included 15 leaves of different plant. The leaves were the first two fully developed ones from the top.

Chl fluorescence parameter analysis: The fluorescence parameters of functional leaves were measured by a pocket fluorometer (*Handy PEA, Hansatech*, UK) according to methods of Strasser *et al*. (1995). The experiment was performed in the morning (07:30–11:30 h); flag leaves were dark-adapted for at least 30 min before measurements and then exposed to continuous red light (peak at 650 nm) for 1 s at 3,000 μmol(photon) m^{-2} s^{-1} with a duration of 800 ms. The experiment was carried out in triplicates and each replicate included 15 leaves of different plants. The performance index on absorption basis (PI_{ABS}) was calculated as:

$$PI_{ABS} = (RC/ABS) \times [\varphi P_0/(1 - \varphi P_0)] \times [\psi_0/(1 - \psi_0)].$$

Protein extraction and sodium dodecyl sulfate-polyacrylamide gel electrophoresis (SDS-PAGE): SDS-PAGE of polypeptides of thylakoid membranes was based on the method described by Ma *et al*. (2016). Proteins were extracted in cool extraction medium (50 mM Tris-HCl, pH = 7.6, 5 mM $MgCl_2$, 10 mM NaCl, 0.4 M sucrose, and 0.1% BSA) and mixed with SDS-loading buffer. The samples were then boiled for 5 min, and equal amounts of proteins were loaded onto 12% polyacrylamide gel. The gel was ran at 120 V, and protein bands were detected using *Coomassie Brilliant Blue R-250* staining.

Western blot analysis: The thylakoid membrane proteins of leaves were extracted according to a previous method (Kang *et al*. 2012). The protein content was determined spectrophotometrically (*Cintra 1010*, *GBC*, Australia) using BSA standard as a reference. About 20 mg of proteins were mixed with loading buffer (250 mM Tris-HCl, pH = 6.8, 50% glycerol, 10% SDS, 5% 2-mercaptoethanol, 0.5% bromophenol blue). This mixture was boiled for 5 min and loaded onto a 12% SDS-PAGE gel, then transferred to PVDF membrane, and immunoblotted with antibodies (RbcL, D1, D2, Lhcb1, Lhcb2, Lhcb3, PsaA, PsaB, Lhca1, Lhca2, Lhca3, PsbQ, PsbO, and PsbP), which were purchased from *Agrisera*, Sweden. Antibodies were detected using a chemiluminescence detection system (*ECL*, *Vazyme*, China).

Statistical analyses were carried out using *SPSS* statistical package, version *17.00* (*SPSS Inc*., Chicago, USA). Parametric one-way analysis of variance (*ANOVA*) was used to assess data. Differences were considered significant at $P<0.05$. Data were expressed as mean ± standard deviation (SD) from at least three individual experiments.

Results

Defective photosynthetic pigmentation and chloroplast development in 812HS: The leaf tip in 812HS exhibited a yellow phenotype (Fig. 1*A*). Elevated Chl *a*/*b* ratios were observed on 4 August, 2014 (44 days after the beginning of experiment) at the jointing stage; the 812HS mutant showed 21% reduction in Chl compared with that in 812S (Fig. 2*A*).

The yellow coloration of 812HS leaves was evaluated by testing the response of 812HS to different light treatments. After the rainy season, the tip of shaded 812HS leaves remained green, while the leaves exposed to natural light turned yellow. No significant difference was observed in 812S leaves exposed to similar conditions (Fig. 1*B*). This observation directly suggested that the yellowing of 812HS was light-induced and the mutation enhanced the photosensitivity of rice leaves.

In order to investigate a role of 812HS mutation in chloroplast development, we compared the ultrastructure of plastids in the 812HS mutant and wild-type plants at different developmental stages by using TEM. The 812S chloroplasts exhibited an orderly arrangement of granal and stromal thylakoids on 23 June (Fig. 3*A*,*B*). The number and volume of starch granules increased in 812S (Fig. 3*C*), while the chloroplasts in 812HS leaves appeared to be spherical on 14 July (Fig. 3*D*). They displayed well-developed membrane systems with grana connected by stromal lamellae (Fig. 3*E*). The stacks of grana in the 812HS mutant appeared loose (Fig. 3*F*) and lacking

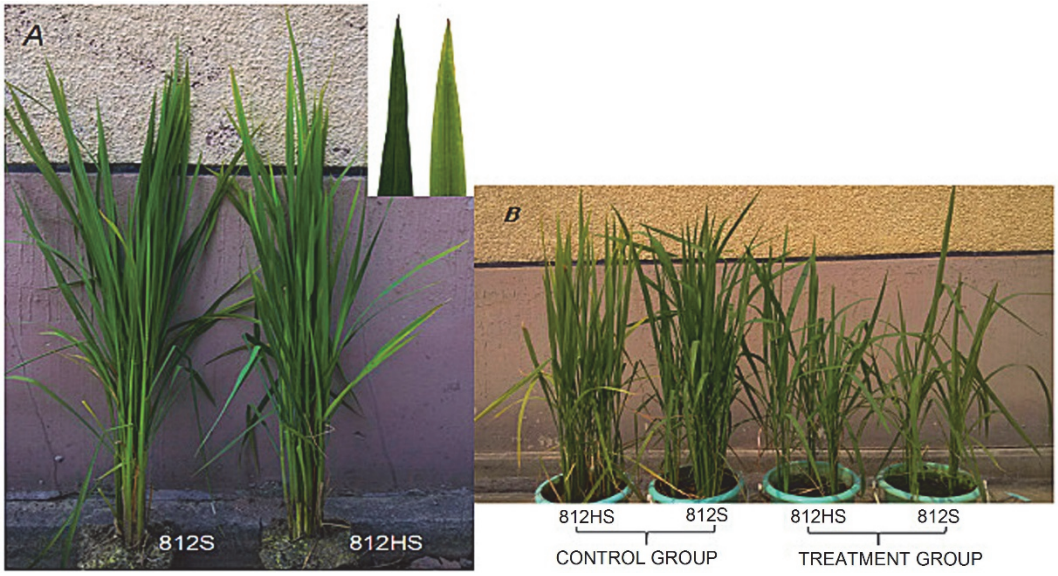

Fig. 1. Phenotypic analysis of the rice mutant 812HS and its wild type 812S (*A*) under natural light in field and (*B*) partial shading in pots.

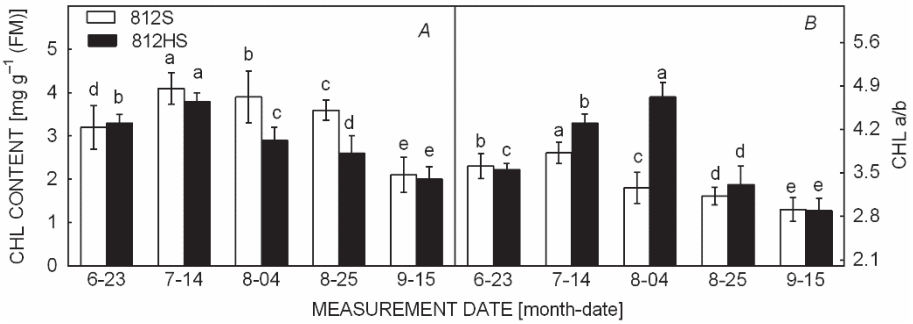

Fig. 2. Effects of photooxidation on photosynthetic pigments (*A*) and chlorophyll (Chl) *a*/*b* (*B*) in the rice mutant 812HS. Data are means ± SD ($n = 3$). Different *small letters* indicate significant differences $p<0.05$, using the *t*-test.

granal membranes and starch granules as compared with the wild type (Fig. 3*F*). At the mature stage on 25 August, numerous osmiophilic drops were seen in the 812HS and 812S (Fig. 3*G*,*H*), and at senescence stage on 4 September, the inner structure of the chloroplast was disorganized and the outer membrane of some chloroplasts was broken (Fig. 3*I*,*J*).

H_2O_2 and $O_2^{\cdot-}$ in the leaves: NBT- and DAB-staining showed specific localization of H_2O_2 and $O_2^{\cdot-}$ (Fig. 4*A,B*). On 23 June, a little staining was observed in 812HS and 812S, and there was no obvious difference between them. With the increased light intensity, the leaves of 812HS showed greater accumulation of H_2O_2 than that in 812S (Fig. 4*A*). Simultaneously, the leaves showed a similar trend of $O_2^{\cdot-}$ accumulation (Fig. 4*B*). As shown by the above histochemical localization, the spectrophotometric quantitation also showed a similar trend in the content of H_2O_2 and $O_2^{\cdot-}$ (Fig. 4*C,D*). On 23 June, there was no difference between 812HS and 812S. However, on 4 August, the H_2O_2 and $O_2^{\cdot-}$ contents increased significantly, especially in 812HS; both contents increased by 46.1% and 43.9%, respectively, over that of 812S.

MDA content: The lipid peroxidation in plants was evaluated by the MDA content. Compared with 812S, photooxidation led to a rapid increase in MDA contents in the leaves of 812HS on 4 August (Fig. 1S, *supplement available online*), peaking at 56.9%.

ROS-scavenging enzymes: The photooxidative effects stimulated activities of antioxidant enzymes (Fig. 5). The SOD activity changed, specifically, on 4 August, resulting in a significant increase in activity (Fig. 5*A*). The POD activity of 812HS was not initially different from that of 812S on 23 June. Later, it was significantly 27.4% higher than that of 812S (Fig. 5*B*). CAT activity in 812HS showed a strong increase representing 7.6% and 10.2% of that in 812S on 23 June and 4 August, respectively (Fig. 5*C*). Subsequently, CAT activity decreased both in 812S and

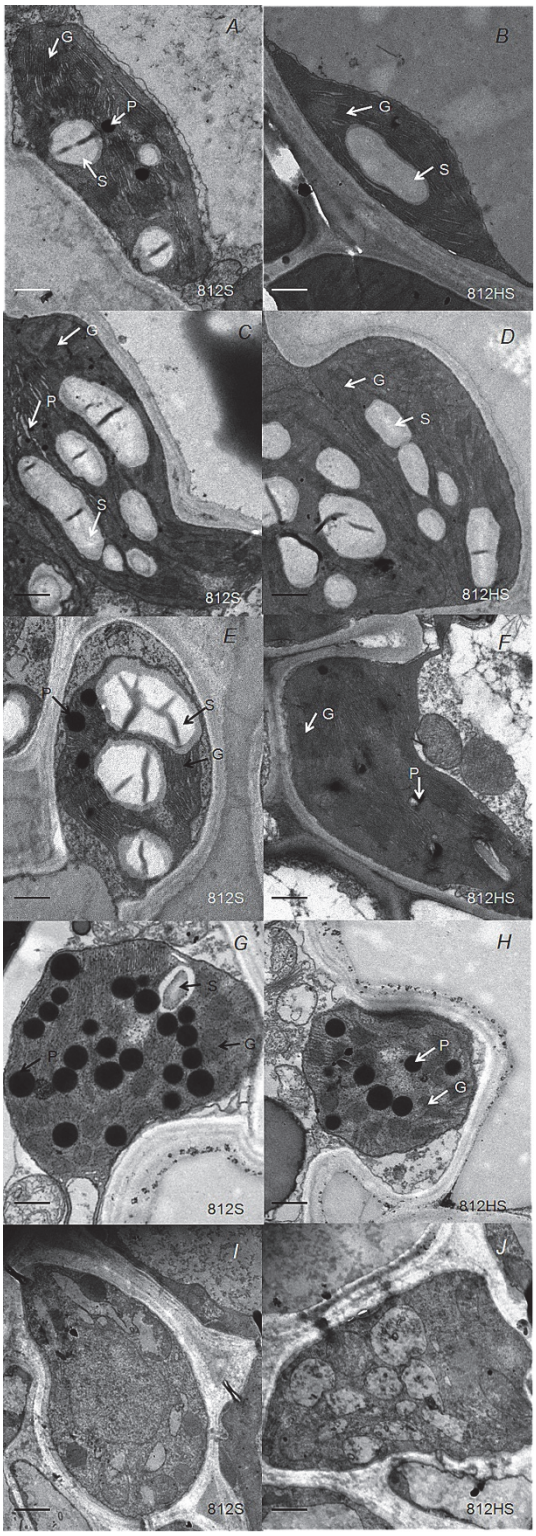

Fig. 3. Effects of photooxidation on the ultrastructure of chloroplasts in the rice mutant 812HS: *A, C, E, G,* and *I*, chloroplasts of the first leaf on 23 June, 14 July, 4 August, 25 August, and 14 September in 812S, respectively. *B, D, F, H*, and *J* chloroplasts of the first leaf on 23 June, 14 July, 4 August, 25 August, and 14 September in 812HS, respectively. Grana thylakoids (g), plastoglobule (p), and stroma lamellae (s). Bar equals 1 μm.

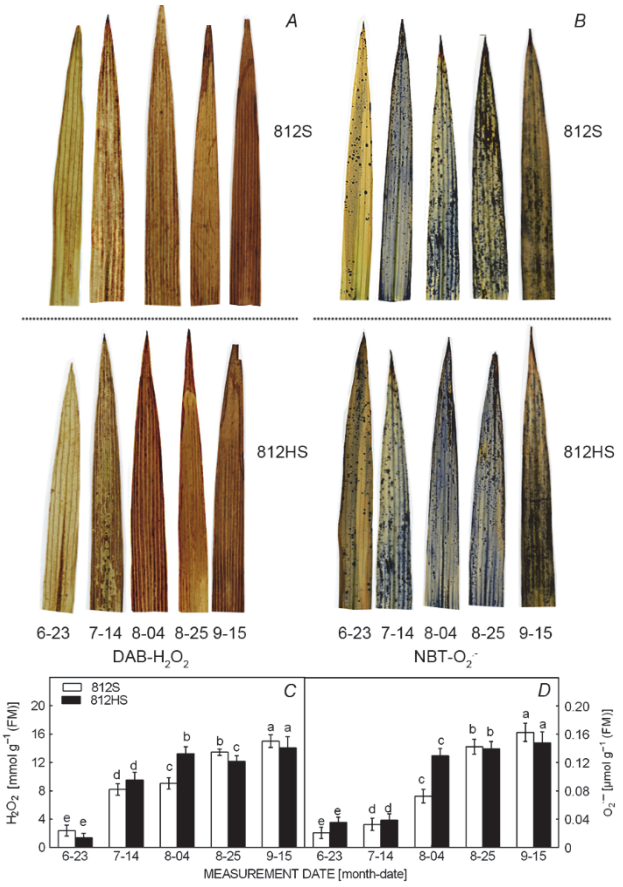

Fig. 4. Histochemical localization of H_2O_2 (*A*) and $O_2^{\cdot-}$ (*B*) in rice leaves. The leaves were infiltrated with DAB staining for H_2O_2 or NBT staining for $O_2^{\cdot-}$, respectively. The content of H_2O_2 (*C*) and $O_2^{\cdot-}$ (*D*) in the leaves of rice mutant 812HS and its wild type 812S. Data are means ± SD (n = 3). Different *small letters* indicate significant differences $p<0.05$, using the *t*-test.

812HS (Fig. 5*C*). The APX and GR activities in 812HS increased from 23 July to 4 August, and they declined subsequently, while the activities of APX and GR reached a peak on 25 August in 812S (Fig. 5*D,E*).

Photophosphorylation activity, ATP content, Ca^{2+}-ATPase and Mg^{2+}-ATPase activities, gas exchange and Chl *a* fluorescence parameters in 812HS: In order to further elucidate changes in primary photochemical reactions, the photophosphorylation activity, ATP content, and Ca^{2+}-ATPase and Mg^{2+}-ATPase activities were investigated using isolated chloroplasts. The photophosphorylation activity and ATP content of the 812HS exhibited a similar trend, namely increase until 14 July and then decreased significantly (Fig. 6*A,B*). Ca^{2+}-ATPase and Mg^{2+}-ATPase activities exhibited the similar trend as photophosphorylation activity and ATP content (Fig. 6*C,D*). On 23 June, P_N showed no significant difference between 812HS and 812S, while it sharply decreased on 4 August in 812HS as compared with 812S (Fig. 7*A*). From the Fig. 7*B*, we found that C_i increased by 55.7% in 812HS as

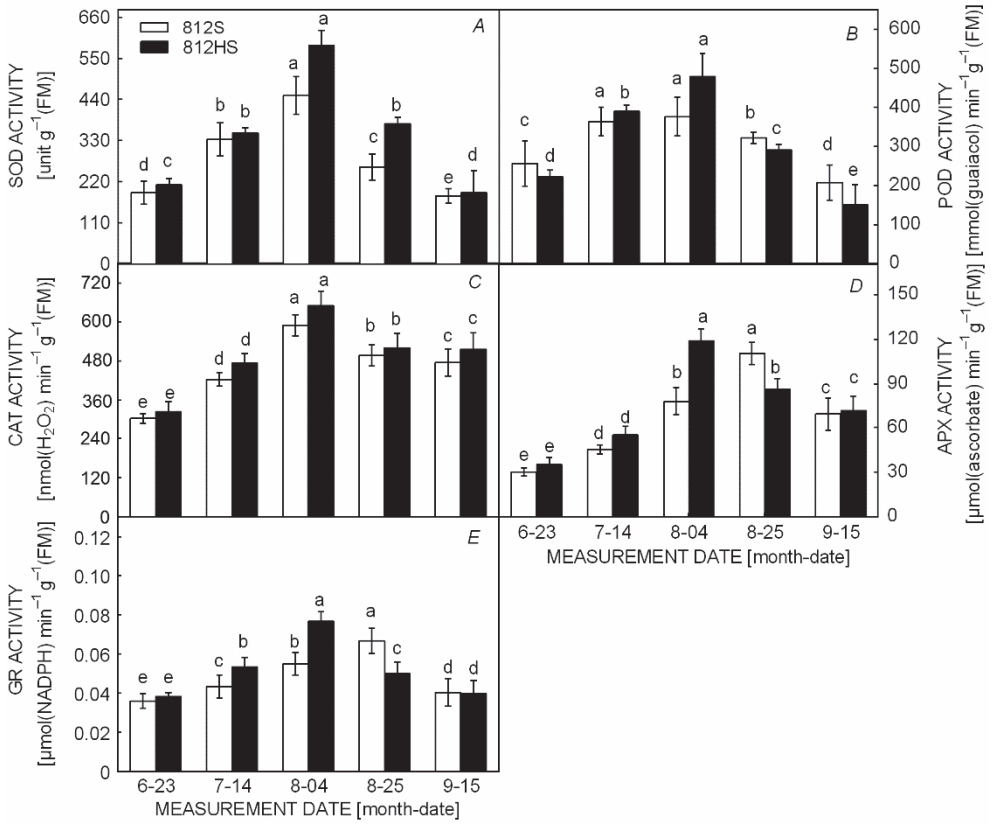

Fig. 5. Effects of photooxidation on the antioxidant enzymes superoxide dismutase (SOD, *A*), peroxidase (POD, *B*), catalase (CAT, *C*), ascorbate peroxidase (APX, *D*), and glutathione reductase (GR, *E*) in the 812HS. Data represent means ± SD (n = 3). Different *small letters* indicate significant differences (p<0.05), using the *t*-test.

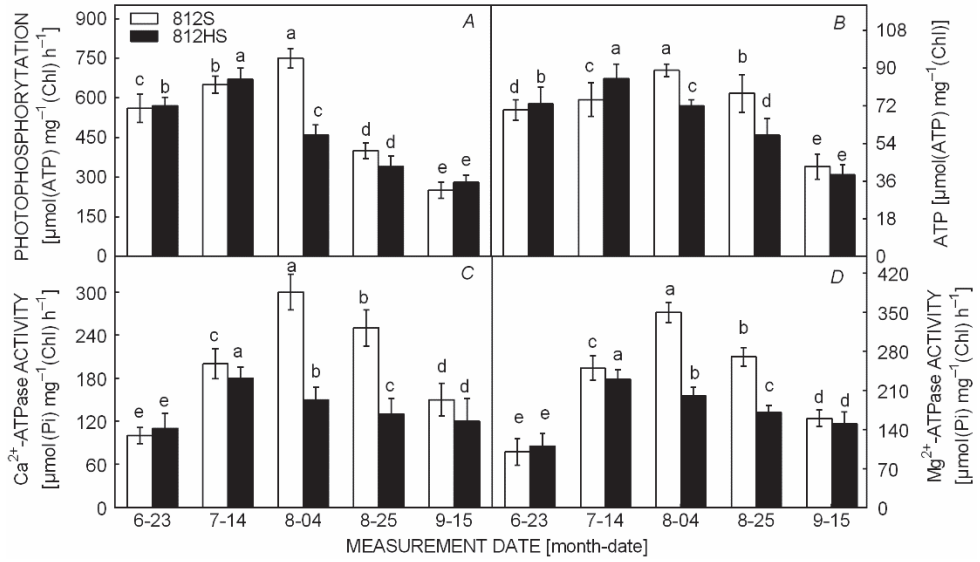

Fig. 6. Effects of photooxidation on photophosphorylation (*A*), ATP content (*B*), Ca^{2+}-ATPase activity (*C*) and Mg^{2+}-ATPase activity (*D*) in 812HS. Data are means ± SD (n = 3). Different *small letters* indicate significant differences (p<0.05), using the *t*-test.

compared with 812S. The value of performance index (PI_{ABS}) was used to evaluate the PSII behavior. PI_{ABS} increased on 14 July, while it declined on 4 August in 812HS (Fig. 7*D*). Maximal quantum yield of PSII (F_V/F_M) showed the similar tendency as that of PI_{ABS} (Fig. 7*C*).

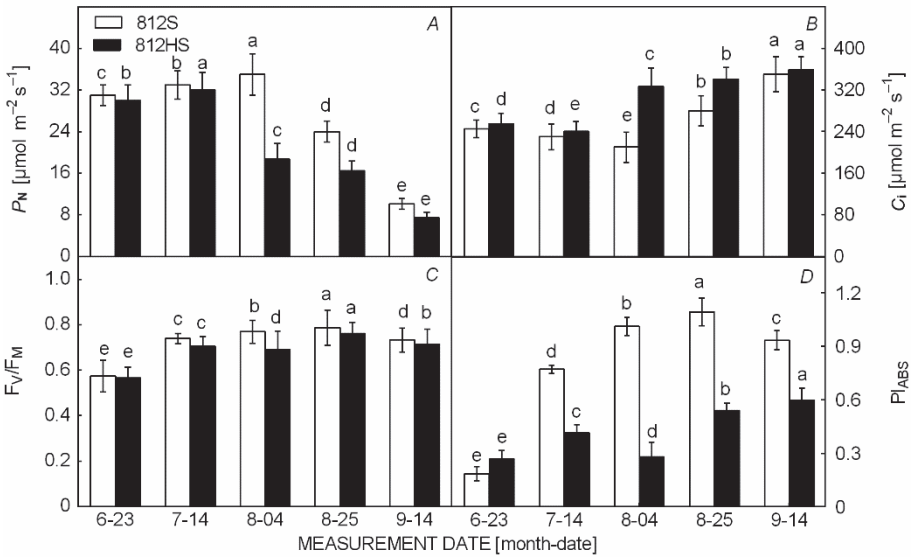

Fig. 7. Effects of photooxidation on net photosynthetic rate (P_N, *A*), intercellular CO_2 concentration (C_i, *B*), maximal quantum yield of PSII (F_V/F_M, *C*), and performance index (PI_{ABS}, *D*) in leaves of 812HS and 812S. Data are means ± SD (n = 15). Different *small letters* indicate significant differences (p<0.05), using the *t*-test.

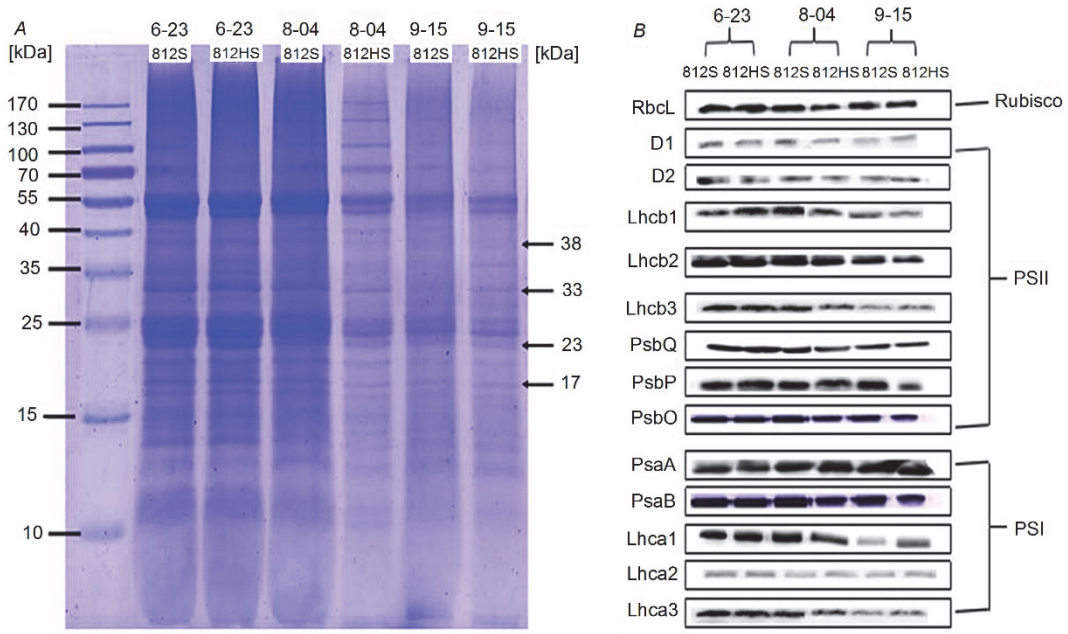

Fig. 8. Effects of photooxidation on protein in 812HS. (*A*) Decreased protein contents after photooxidation of leaves in 812HS by SDS-PAGE. (*B*) Immunoblot with antibodies against photosynthesis-associated proteins of thylakoids isolated from leaves of rice in 812HS. Each lane was loaded with similar amounts of proteins.

Photosynthesis-related proteins: SDS-PAGE of total protein extracts from the leaves of 812HS and 812S showed that photooxidation induced a marked decline in protein contents on 4 August (Fig. 8*A*). The contents of four polypeptides with apparent molecular mass of 38, 33, 23, and 17 kDa starkly diminished in response to photooxidation. On 15 September, the protein content was not significantly different between 812HS and 812S. Immunoblotting revealed that the oxygen-evolving complex (PsbP, PsbO, and PsbQ) declined in addition to the core proteins of PSII (D1, D2) as well as Lhcb1, 2, 3 on 4 August in 812HS. The decline in the relative content of Rubisco large subunit was also significant. The PSI core complexes and LHCI showed a relatively slower decline on 4 August in 812HS compared with 812S (Fig. 8).

Discussion

Ultrastructure of chloroplasts: Our study showed that photooxidation distinctly affected the Chl content, photosynthetic parameters, and chloroplast development in 812HS (Figs. 2,3,6). Photosynthetic pigment content represents a sensitive parameter under stress conditions and is used as a potential biomarker of abiotic stress (Ma *et al*. 2015). The Chl content in the leaves of 812HS decreased and the Chl *a*/*b* ratio was the highest on 4 August compared with that of 812S (Fig. 2*A,B*). The decreased Chl content induced by photooxidation might be attributed to inhibition of the Chl biosynthesis (Ranjbarfordoei *et al*. 2011) or effects on the enzymes involved in Chl biosynthesis pathway (Singh *et al*. 2006, Sivaci *et al*. 2008). The increased Chl *a*/*b* ratio showed that the Chl *b* synthesis was likely inhibited more than that of Chl *a* (Wu *et al*. 2007).

Further, photooxidation apparently damaged the chloroplast ultrastructure (Fig. 3*F*). Observations on 23 July revealed normal chloroplast ultrastructure in 812HS and 812S (Fig. 3*A,B*). Due to the rainy season, significant alterations in chloroplast ultrastructure occurred in 812HS, especially on 4 August (Fig. 3*D*), which was accompanied by the increasing number and size of translucent plastoglobuli. Ladygin (2004) reported that lipid components of membranes, which were synthesized but not utilized in thylakoid biosynthesis, were partially conserved as plastoglobuli. Hence, plastoglobuli in chloroplasts are deemed to contain components from disintegrated thylakoid membranes. Altered thylakoid membrane structure may directly affect membrane functionality and inhibit photosynthesis when the integrity of the chloroplast ultrastructure in cells is destroyed under environmental stress (Chen *et al*. 2004). These changes were similar to the disorganization of thylakoid membranes observed in *Ocimum basilicum* (Bishehkolaei *et al*. 2011). Changes in chloroplast ultrastructure are another important reason for the decrease in Chl content. Thus, the loss of pigments and damage to the chloroplasts ultimately disturbed photosynthetic capacity (Qiao *et al*. 2013).

Antioxidant enzyme systems of 812HS: Abiotic stress triggers oxidative damage resulting from the production of ROS (Alcázar *et al*. 2010). $O_2^{\cdot-}$ and H_2O_2 contents in leaves of 812HS on 4 August increased gradually with photooxidation (Fig. 4*C,D*), which was consistent with previous findings (Zhang *et al*. 2009). This effect was also evidenced by the decline in photosynthetic pigments (Fig. 2*A*) and proteins (Fig. 7). MDA is a common product of polyunsaturated fatty acid peroxidation in biomembranes. As shown in Fig. 1S, MDA contents prominently increased in 812HS on 4 August, suggesting that photooxidation of the cell membrane induced oxidative stress and it was related to the production of $O_2^{\cdot-}$ and H_2O_2 (Wang *et al*. 2008) in agreement with the report on *Populus cathayana* by Zhao *et al*. (2009). $O_2^{\cdot-}$ and H_2O_2 enhanced oxidative and lipid peroxidation, increased MDA content, damaged cellular membrane, chloroplast structures, and their function. It invariably disturbed metabolic processes, and finally inhibited the growth. In order to avoid oxidative damage by ROS, antioxidants, including key enzymes (*i.e*., SOD, POD, CAT, APX, and GR) catalyze ROS detoxification (Vuleta *et al*. 2016). In our study, the activities of SOD in 812HS and 812S increased upon exposure to high light on 4 August, especially in 812HS. However, the production of $O_2^{\cdot-}$ in 812HS was far higher on 4 August than that in 812S (Fig. 4*D*), probably because the increased $O_2^{\cdot-}$ production rate exceeded the SOD ability to remove $O_2^{\cdot-}$ (Qiao *et al*. 2013). Such results indicate that stress tolerance of plants depends on the equilibrium between the production of ROS and the antioxidant activity (Xu *et al*. 2010). In addition, the activities of SOD decreased during senescence on 15 September (Fig. 5*A*). It suggests that the antioxidant enzyme system of rice lost its intrinsic balance and was unable to resist effectively to the further generation of excess ROS. Further, POD, CAT, APX, and GR activities also increased slightly in 812HS leading to H_2O_2 accumulation, evidenced by the damaged structure of chloroplast membranes and pathophysiology (Figs. 3,6,7). Ultimately, these changes resulted in severe photooxidation of 812HS, which was consistent with a previous study (Zhang *et al*. 2009). These relationships appear to be mediated by specific gene expression, which needs additional investigations.

Energy imbalance and photosynthesis: Photophosphorylation in chloroplasts produces ATP and transfers light energy to chemical energy in a reaction catalyzed by ATP-synthase located in chloroplast thylakoid membranes (Ma *et al*. 2016). Photophosphorylation sharply decreased on 4 August in 812HS as well as the capacity of chloroplasts to produce ATP and transform light energy into chemical energy (Fig. 6*A*,*B*), which was confirmed by the variation in Ca^{2+}-ATPase and Mg^{2+}-ATPase activities (Fig. 6*C*,*D*). Abiotic stressors, such as photooxidation, also affect plants by altering soluble protein contents (Yang *et al*. 2011). In our present investigation, the protein content decreased dramatically in the leaves of 812HS on 4 August. SDS-PAGE also revealed that photooxidation decreased the amount of proteins (Fig. 8*A*) in order to avoid energy imbalance when light exceed the requirement. It may be due to an increase in protease activity leading to a decrease in protein content (Xu *et al*. 2010). In addition, the main reduction in four polypeptides with apparent molecular mass of 38, 33, 23, and 17 kDa, which are the protein subunits of the PSII oxygen-evolving complex, demonstrated that the PSII oxygen-evolving complex was most likely damaged under photooxidation. The immunoblot analysis confirmed the decline in PsbP, PsbO, and PsbQ contents. The core proteins of PSII (D1,

D2) as well as Lhcb1, 2, and 3 also declined in parallel on 4 August in 812HS. The decline in the relative content of Rubisco large subunit was also significant. The PSI core complexes and LHCI showed a slower decline on 4 August in 812HS compared with 812S (Fig. 8*B*). We supposed that the decreased LHCII subunits in leaf under photooxidation hampered the light-harvesting capacity, and was an adaptation in order to balance the light energy absorption with CO_2 assimilation (Wang *et al*. 2014). To avoid the energy imbalance resulting from photooxidation, plants downregulate protein contents associated with photosynthetic light harvesting to reduce the light energy absorbed. The decline in the core proteins of PSII (D1, D2) indicated serious photooxidative damage. Based on these results, it was suggested that this should promote thermal dissipation, and prevent excessive energy from the plant. Guha *et al*. (2013) deemed that this was a photoprotection strategy of rice from the overreduction of the electron transport chain and strengthen dissipation of excessive energy for the purpose of minimizing photooxidative damage in the thylakoid membrane. Simultaneously, P_N is an important indicator which can reflect the photosynthetic capacity of plants. In our study, it sharply decreased and C_i significantly increased on 4 August in 812HS as compared with 812S (Fig. 7*A,B*). Photooxidation has harmful effects on leaves, which was indicated by F_V/F_M and PI_{ABS}. The values of F_V/F_M reflect the potential quantum efficiency of PSII and are used as a sensitive indicator of plant photosynthetic performance. Li *et al*. (2010) suggested that F_V/F_M is particularly useful to determine thermal, salinity, dessication, and other environmental stressors, as a robust indicator of photosynthetic stress. In our study, F_V/F_M increased on 14 July, and sharply decreased on 4 August in 812HS (Fig. 7*C*). The performance index (PI_{ABS}) is applied to quantify the PSII behavior. It can more precisely reflect the state of the plant photosynthetic apparatus and is more sensitive than F_V/F_M to certain stresses (Van Heerden *et al*. 2004). PI_{ABS} increased during the whole growth period in 812S (Fig. 7*D*). Our results indicated that the leaves of 812HS were sensitive to high light intensity and their photosynthetic efficiency decreased.

References

Alcázar R., Altabella T., Marco F. *et al*.: Polyamines: molecules with regulatory functions in plant abiotic stress tolerance. – Planta **231**: 1237-1249, 2010.

Bishehkolaei R., Fahimi H., Saadatmand S. *et al*.: Ultrastructural localisation of chromium in *Ocimum basilicum*. – Turk. J. Bot. **35**: 261-268, 2011.

Blokhina O., Virolainen E., Fagerstedt K.V.: Antioxidants, oxidative damage and oxygen deprivation stress: a review. – Ann. Bot.-London **91**: 179-194, 2003.

Fang J., Chai C.L, Qian Q. *et al.*: Mutations of genes in synthesis of the carotenoid precursors of ABA lead to pre-harvest sprouting and photo-oxidation in rice. – Plant J. **54**: 177-189, 2008.

Foyer C.H., Lopez-Delgado H., Dat J.F. *et al*.: Hydrogen peroxide- and glutathione-associated mechanisms of acclimatory stress tolerance and signalling. – Physiol. Plantarum **100**: 241-254, 1997.

Fu Y.Y., Li F.F., Xu T. *et al*.: Bioaccumulation, subcellular, and molecular localization and damage to physiology and ultrastructure in *Nymphoides peltata* (Gmel.) O. Kuntze exposed to yttrium. – Environ. Sci. Pollut. R. **21**: 2935-2942, 2014.

Gratão P.L., Polle A., Lea P.J. *et al*.: Making the life of heavy metal stressed plants a little easier. – Funct. Plant Biol. **32**: 481-494, 2005.

Guha A., Sengupta D., Reddy A.R.: Polyphasic chlorophyll *a* fluorescence kinetics and leaf protein analyses to track dynamics of photosynthetic performance in mulberry during progressive drought. – J. Photoch. Photobio. B. **119**: 71-83, 2013.

Hossain M.A., Hasanuzzaman M., Fujita M.: Up-regulation of antioxidant and glyoxalase systems by exogenous glycinebetaine and proline in mung bean confer tolerance to cadmium stress. – Physiol. Mol. Biol. Plants **16**: 259-272, 2010.

Chen G.X., Liu S.H., Zhang C.J. *et al*.: Effects of drought on photosynthetic characteristics of flag leaves of a newly-developed super-high-yield rice hybrid. – Photosynthetica **42**: 573-578, 2004.

Kang Z., Li G., Huang J. *et al.*: Photosynthetic and physiological analysis of the rice high-chlorophyll mutant (Gc). – Plant Physiol. Bioch. **60**: 81-87, 2012.

Ketcham S.R., Davenport J.W., Warncke K.*et al*: Role of the gamma subunit of chloroplast coupling factor 1 in the light-dependent activation of photophosphorylation and ATPase activity by dithiothreitol. – J. Biol. Chem. **259**: 7286-7293, 1984.

Ladygin V.G.: Photosystem damage and spatial architecture of thylakoids in chloroplasts of pea chlorophyll mutants. – Biol. Bull+ **31**: 268-276, 2004.

Lai D., Xia S.J., Lv C.G. *et al*.: Mapping a leaf photo-oxidation gene *LPO1(t)* in rice. – Jiangsu Agric. Sci. **28**: 1212-1217, 2012.

Li G., Wan S., Zhou J. *et al*.: Leaf chlorophyll fluorescence, hyperspectral reflectance, pigments content, malondialdehyde and proline accumulation responses of castor bean (*Ricinus communis* L.) seedlings to salt stress levels. – Ind. Crop. Prod. **31**: 13-19, 2010.

Long S.P., East T.M., Baker N.R.: Chilling damage to photosynthesis in young *Zea mays*: 1. effects of light and temperature variation on photosynthetic CO_2 assimilation. – J. Exp. Bot. **34**: 177-188, 1983.

Ma J., Lv C.F., Xu M.L. *et al*.: Photosynthesis performance, antioxidant enzymes, and ultrastructural analyses of rice seedlings under chromium stress. – Environ. Sci. Pollut. R. **23**: 1768-1778, 2016.

Nakano Y., Asada K.: Purification of ascorbate peroxidase in spinach chloroplasts: its inactivation in ascorbate depleted medium and reactivation by monodehydro ascorbate radical. – Plant Cell Physiol. **28**: 131-140, 1987.

Phung T. H., Jung S.: Differential antioxidant defense and detoxification mechanisms in photodynamically stressed rice plants treated with the deregulators of porphyrin biosynthesis, 5-aminolevulinic acid and oxyfluorfen. – Biochem. Bioph. Res.

Co. **459**: 346-351, 2015.
Qiao X.Q., Shi G.X., Chen L. *et al*.: Lead-induced oxidative damage in steriled seedlings of *Nymphoides peltatum*. – Environ. Sci. Pollut. R. **20**: 5047-5055, 2013.
Ranjbarfordoei A., Samson R., Van Damme P.: Photosynthesis performance in sweet almond [*Prunus dulcis* (Mill) D. Webb] exposed to supplemental UV-B radiation. – Photosynthetica **49**: 107-111, 2011.
Rao M.V., Paliyath G., Ormrod D.P.: Ultraviolet-B-and ozone-induced biochemical changes in antioxidant enzymes of *Arabidopsis thaliana*. – Plant Physiol. **110**: 125-136, 1996.
Rossel J.B., Wilson P.B., Hussain D. *et al*.: Systemic and intracellular responses to photooxidative stress in *Arabidopsis*. – Plant Cell **19**: 4091-4110, 2007.
Sandalio L.M., Dalurzo H.C., Gómez M. *et al*.: Cadmium-induced changes in the growth and oxidative metabolism of pea plants. – J. Exp. Bot. **52**: 2115-2126, 2001.
Shah K., Kumar R.G., Verma S. *et al*.: Effect of cadmium on lipid peroxidation, superoxide anion generation and activities of antioxidant enzymes in growing rice seedlings. – Plant Sci. **161**: 1135-1144, 2001.
Sharma P., Dubey R.S.: Involvement of oxidative stress and role of antioxidative defense system in growing rice seedlings exposed to toxic concentrations of aluminium. – Plant Cell Rep. **26**: 2027-2038, 2007.
Shen W.J., Chen G.X., Xu J.G., *et al*.: High light acclimation of *Oryza sativa* L. leaves involves specific photosynthetic-sourced changes of NADPH/$NADP^+$ in the midvein. – Protoplasma **252**: 77-87, 2015.
Singh S., Eapen S., D'Souza S.F.: Cadmium accumulation and its influence on lipid peroxidation and antioxidative system in an aquatic plant, *Bacopa monnieri* L. – Chemosphere **62**: 233-246, 2006.
Sivaci A., Elmas E., Gümüş F. *et al*.: Removal of cadmium by *Myriophyllum heterophyllum* Michx. and *Potamogeton crispus* L. and its effect on pigments and total phenolic compounds. – Arch. Environ. Con. Tox. **54**: 612-618, 2008.
Stewart R.R.C., Bewley J.D.: Lipid peroxidation associated with accelerated aging of soybean axes. – Plant Physiol. **65**: 245-248, 1980.
Strasser R.J., Srivastava A., Govindjee.: Polyphasic chlorophyll *a* fluorescence transient in plants and cyanobacteria. – Photochem. Photobiol. **61**: 32-42, 1995.
Szabó I., Bergantino E., Giacometti G.M.: Light and oxygenic photosynthesis: energy dissipation as a protection mechanism against photo-oxidation. – EMBO Rep. **6**: 629-634, 2005.
Vallejos R.H., Arana J.L., Ravizzini R.A.: Changes in activity and structure of the chloroplast proton ATPase induced by illumination of spinach leaves. – J. Biol. Chem. **258**:7317-7321, 1983.
Van Heerden P.D.R., Strasser R.J., Krüger G.: Reduction of dark chilling stress in N_2-fixing soybean by nitrate as indicated by chlorophyll a fluorescence kinetics. – Physiol. Plantarum **121**: 239-249, 2004.
Vuleta A., Jovanović S. M., Tucić B.: Adaptive flexibility of enzymatic antioxidants SOD, APX and CAT to high light stress: The clonal perennial monocot *Iris pumila* as a study case. – Plant Physiol. Bioch. **100**: 166-173, 2016.
Wang C., Wang X., Tian Y.: Oxidative stress and potential biomarkers in tomato seedlings subjected to soil lead contamination. – Ecotox. Environ. Safe. **71**: 685-691, 2008.
Wang Y., Jiang X., Li K. *et al*: Photosynthetic responses of *Oryza sativa* L. seedlings to cadmium stress: physiological, biochemical and ultrastructural analyses. – BioMetals **27**: 389-401, 2014.
Wu Z.M., Zhang X., He B. *et al.*: A chlorophyll-deficient rice mutant with impaired chlorophyllide esterification in chlorophyll biosynthesis. – Plant Physiol. **145**: 29-40, 2007.
Xu Q.S., Hu J.Z., Xie K.B. *et al*.: Accumulation and acute toxicity of silver in *Potamogeton crispus* L. – J. Hazard Mater. **173**:186-193, 2010.
Yang Y.L., Zhang Y.Y., Wei X.L. *et al*.: Comparative anti-oxidative responses and proline metabolism in two wheat cultivars under short term lead stress. – Ecotox. Environ. Safe. **74**: 733-740, 2011.
Zhang S.S., Zhang H.M., Qin R. *et al*.: Cadmium induction of lipid peroxidation and effects on root tip cells and antioxidant enzyme activities in *Vicia faba* L. – Ecotoxicology **18**: 814-823, 2009.
Zhao H.X., Yan L., Duan B. *et al*.: Sex-related adaptive responses of *Populus cathayana* to photoperiod transitions. – Plant Cell Environ. **32**: 1401-1411, 2009.
Zhou Y., Gong Z., Yang Z. *et al*.: Mutation of the light-induced yellow leaf 1 gene, which encodes a geranylgeranyl reductase, affects chlorophyll biosynthesis and light sensitivity in rice. – PLoS One **8**: e75299, 2013.
Zhu X.Y., Chen G.C., Zhang C.L.: Photosynthetic electron transport, photophosphorylation, and antioxidants in two ecotypes of reed (*Phragmites communis* Trin.) from different habitats. – Photosynthetica **39**: 183-189, 2001.